Supplementary material for:

Analysis of Hedgehog Signaling in Cerebellar Granule Cell Precursors in a Conditional *Nsdhl* Allele Demonstrates an Essential Role for Cholesterol in Postnatal CNS Development

David Cunningham[1], Andrea E. DeBarber[2], Natalie Bir[1], Laura Binkley[1], Louise S. Merkens[3], Robert D. Steiner[3,4,5,6], and Gail E. Herman[1,*]

[1]Center for Molecular and Human Genetics, The Research Institute at Nationwide Children's Hospital and Department of Pediatrics, The Ohio State University, Columbus, OH
[2]Departments of Physiology and Pharmacology, [3]Pediatrics and [4]Molecular and Medical Genetics, and [5]Institute on Development and Disability, Doernbecher Children's Hospital, Oregon Health & Science University, Portland, OR
[5]Marshfield Clinic Research Foundation and the Department of Pediatrics, University of Wisconsin School of Medicine and Public Health, Marshfield and Madison, WI

*To whom correspondence should be addressed at
Gail E. Herman, MD/PhD
Professor, Center for Molecular and Human Genetics
The Research Institute at Nationwide Children's Hospital
and Department of Pediatrics, The Ohio State University
700 Children's Dr. Rm W403, Columbus, OH 43205
Phone: 614-722-2848/2849 Fax: 614-722-3330
email: Gail.Herman@NationwideChildrens.org

Supplementary Figure Legends

Figure S1. **(A)** NSDHL immunostaining of *Nsdhl*^{flx5}/Y and *Nsdhl*$^{\Delta 5}$/Y E10.5 embryos from an *Nsdhl*$^{flx5/flx5}$ x *Sox2*-cre cross. Scale bar: 1mm. **(B)** A heterozygous *Sox2*-cre/*Nsdhl*$^{\Delta 5/+}$ P11 female (arrow) with two *Nsdhl*$^{flx5/+}$ littermates. The phenotype of the affected female was indistinguishable from a *Bpa*^{1H}/+ P11 female **(C)**, including patches of hyperkeratotic, hairless skin, skeletal abnormalities and a smaller size than wild type littermates. **(D)** Growth curves from P3 to P12 of *Nsdhl*^{flx5}/Y and *Nsdhl*$^{\Delta 5}$/Y male pups from an *Nsdhl*$^{flx5/flx5}$ x *hGFAP*-cre cross. Each data point is the mean (±SEM) weight of the pups (N = 6 for each genotype).

Figure S2. Histology and NSDHL immunostaining of *Nsdhl*^{flx5}/Y and *Nsdhl*$^{\Delta 5}$/Y brains at P0. **(A, B)** Hematoxylin/eosin staining of sagittal sections showed that the granule neurons in the hippocampus (arrow) of *Nsdhl*$^{\Delta 5}$/Y animals were more dispersed and fewer in number than in the *Nsdhl*^{flx5}/Y brain. **(C-J)** NSDHL immunostaining of P0 brains demonstrated loss of normal NSDHL expression in the hippocampus, cerebral cortex and cerebellum of *Nsdhl*$^{\Delta 5}$/Y pups. Abbreviations: Cb, cerebellum; Cx, cerebral cortex; DG, dentate gyrus; EGL, external granule layer; Hp, hippocampus; OB, olfactory bulb.

Figure S3. Histology and NSDHL immunostaining of *Nsdhl*^{flx5}/Y and *Nsdhl*$^{\Delta 5}$/Y brains at P7. **(A-F)** Hematoxylin/eosin staining of sagittal sections from P7 brains revealed abnormalities in the *Nsdhl*$^{\Delta 5}$/Y cerebellum, hippocampus, and cerebrum. The *Nsdhl*$^{\Delta 5}$/Y cerebellum **(B)** was smaller, with less organized layering of cell types than the *Nsdhl*^{flx5}/Y sample **(A)**. The normal, densely packed organization of granule neurons in the CA regions and dentate gyrus of the hippocampus **(C)** was virtually absent in the *Nsdhl*$^{\Delta 5}$/Y brain **(D)**.The outer layer of the *Nsdhl*$^{\Delta 5}$/Y cerebral cortex showed an increased number of pycnotic nuclei (arrows) **(F)** suggesting abnormal cell death. **(G-J)** NSDHL immunostaining of P7 brains **(G,H)** showed a lack of normal staining in the outer layers of the cerebral cortex, hippocampus and much of the cerebellum, similar to the results from P0 brains. At high magnification **(I)**, (boxed region in panel G**)**, the *Nsdhl*^{flx5}/Y cerebellum showed the expected normal pattern of staining, with the most intense signal present in Bergmann glia (red arrows), and faint staining in Purkinje cells (black arrows) and developing granule neurons of the EGL and IGL. NSDHL expression was maintained in Purkinje cells of the *Nsdhl*$^{\Delta 5}$/Y cerebellum **(J)**, (boxed region of panel H**)**, while no signal was present in the Bergmann glia or granule neurons. Abbreviations: Cb, cerebellum; Cx, cerebral cortex; BG, Bergmann glia; DG, dentate gyrus; EGL, external granule layer; Hp, hippocampus; IGL, inner granule layer; OB, olfactory bulb.

Figure S4. (A) Comparison of Purkinje cell layer (PCL) morphology in *Nsdhl*^{flx5}/Y and *Nsdhl*$^{\Delta 5}$/Y cerebella at P7 by immunohistochemical staining for calbindin. Note the uniform layer of Purkinje cells with developing dendritic arborization at the boundary of the IGL and molecular layer in all of the lobules shown for the *Nsdhl*^{flx5}/Y sample, in contrast to the irregular PCL morphology with poor or absent dendritic arborization in regions of the *Nsdhl*$^{\Delta 5}$/Y cerebellum. Scale bar: 500 μm. **(B)** Immunofluorescent staining for TAG1 and BrdU in the EGL of cerebella from *Nsdhl*^{flx5}/Y and *Nsdhl*$^{\Delta 5}$/Y males at P7. BrdU-positive GCPs define the proliferative oEGL and TAG1 marks postmitotic, differentiating GCPs of the iEGL. While some mutant GCPs became post-mitotic and began to differentiate and migrate, as demonstrated by TAG-1 immunofluorescence, note that both the oEGL (TAG-1 negative) and iEGL (TAG-1 positive), were thinner in the mutant sample at this stage. Scale bar: 100 μm. **(C)** Comparison of cell proliferation in *Nsdhl*^{flx5}/Y and *Nsdhl*$^{\Delta 5}$/Y cerebella at P5 by BrdU incorporation. The samples were labeled with BrdU for 2 h *in vivo* and fixed sections were immunostained for BrdU (see Materials and Methods). Dense labeling was seen throughout the EGL of both *Nsdhl*^{flx5}/Y and *Nsdhl*$^{\Delta 5}$/Y cerebella. However, under high magnification, the mutant sample showed a thinner layer of proliferating cells in the EGL than the control, consistent with the reduced number of PHH3-positive cells shown in Figure 3. **(D)** Comparison of cell proliferation in *Nsdhl*^{flx5}/Y and *Nsdhl*$^{\Delta 5}$/Y cerebella at P7 by BrdU incorporation, as in Panel C. Note the dramatically reduced proportion of BrdU(+) cells in the abnormally thin EGL in the *Nsdhl*$^{\Delta 5}$/Y sample. Abbreviations: EGL, external granule layer; IGL, inner granule layer. The Roman numerals identify specific cerebellar lobules.

Figure S5. Representative GC-FID chromatograms showing sterol profiles for freshly isolated **(A)** and cultured **(B)** GCPs from *Nsdhl*^{flx5}/Y and *Nsdhl*$^{\Delta 5}$/Y cerebella at P7 and P4 respectively. The cultured GCPs were isolated at P4 and maintained in SFM with SHH (1 μg/ml) for 48 h after plating. Cholesterol and desmosterol were reduced in the *Nsdhl*$^{\Delta 5}$/Y samples; however, the ratio of the two compounds in each sample was not statistically different (see Fig. 2E). Peaks representing one or more monomethylsterols were elevated in the isolated and cultured *Nsdhl*$^{\Delta 5}$/Y GCPs, consistent with sterol profiles seen in cultured cells or tissue samples from heterozygous *Bpa*^{1H} females (*Nsdhl* null allele), CK Syndrome patients (hypomorphic *NSDHL* allele) and an *SC4MOL* deficient patient (1-3). **(C)** Representative GC-FID chromatograms for *Nsdhl*^{flx5}/Y and *Nsdhl*$^{\Delta 5}$/Y GCPs cultured in the presence of ketoconazole (2 μM). Note the presence of prominent peaks for lanosterol (derivatized and underivatized) in both samples, resulting from the inhibition of CYP51A1 by ketoconazole. In addition, treatment with ketoconazole reduced the cholesterol concentration in the *Nsdhl*^{flx5}/Y sample to a level similar to the *Nsdhl*$^{\Delta 5}$/Y GCPs, as well as greatly diminished the concentration of the two 4α-methylsterols in the *Nsdhl*$^{\Delta 5}$/Y sample (see Figure 7D). **(D)** Representative GC-mass spectrometry chromatograms for GCPs isolated from *Nsdhl*^{flx5}/Y and *Nsdhl*$^{\Delta 5}$/Y P7 cerebella showing two methylsterol peaks at RT 22.8 and 24.1 in the *Nsdhl*$^{\Delta 5}$/Y sample. Identification of each of the methylsterols by mass spectrum matching to NIST data is shown below.

Figure S6. *Gli1*^{LacZ} reporter expression in *Nsdhl*^{flx5}/Y and *Nsdhl*$^{\Delta 5}$/Y cerebella at P7 assayed by X-gal staining of 60 μm floating sections. X-gal staining was limited to 4 h to avoid saturation of the β-galactosidase signal. The samples were from siblings from two litters. Although the staining pattern was variable among samples, generally more intense and extensive staining was observed in the EGL and Purkinje cell layer (PCL) of the *Nsdhl*^{flx5}/Y samples **(A, C, E)** than in *Nsdhl*$^{\Delta 5}$/Y littermates **(B, D, F)**. The reduced *Gli*1^{LacZ} signal in the *Nsdhl*$^{\Delta 5}$/Y samples is consistent with the ~2-fold lower level of *Gli*1 expression detected by qPCR analysis of RNA from *Nsdhl*$^{\Delta 5}$/Y P6 cerebella compared with *Nsdhl*^{flx5}/Y P6 cerebella (Fig. 6B). The overall pattern of higher *Gli*1^{LacZ} expression in the anterior lobes of the cerebellum at this stage of development is consistent with previous studies (4).

Figure S7. Effects of LDL and/or ketoconazole treatment on cell morphology of *Nsdhl*^{flx5}/Y **(A,C,E,G**) and *Nsdhl*$^{\Delta 5}$/Y **(B,D,F,H)** differentiating GCPs *in vitro*. Under phase contrast microscopy, untreated *Nsdhl*$^{\Delta 5}$/Y GCPs **(B)** displayed small cell bodies surrounding the circular nucleus, with few neurite extensions. Treatment of mutant cells with LDL **(D**) resulted in a more normal, spindle shaped cell body with extensive neurites, similar to untreated *Nsdhl*^{flx5}/Y GCPs (panel A). Although *Nsdhl*$^{\Delta 5}$/Y GCPs treated with ketoconazole **(F)** were not morphologically normal, they did show much more robust neurite outgrowth than the untreated cells (panel B). Scale bar:100 μm.

Figure S8. Effect of exogenous T-MAS on *Nsdhl*^{flx5}/Y GCP morphology *in vitro*. The GCPs were isolated from P4 cerebella and cultured for 48 h with or without added T-MAS that was complexed with fatty acid-reduced bovine serum albumin (FAR-BSA) as a water soluble carrier. Equal amounts of FAR-BSA vehicle were added to all cultures. Cultures were visualized as in Figure S7. The lower concentration of T-MAS (2.5 μg/ml) had little or no visible effect on cell morphology. However, at 10 μg/ml, the exogenous T-MAS resulted in smaller, rounded cell bodies in the *Nsdhl*^{flx5}/Y GCPs, reminiscent of untreated *Nsdhl*$^{\Delta 5}$/Y GCPs (Supplementary material Figure S7A). Scale bar: 100 μm.

References for Supplementary Material

1. Liu, X.Y., Dangel, A.W., Kelley, R.I., Zhao, W., Denny, P., Botcherby, M., Cattanach, B., Peters, J., Hunsicker, P.R., Mallon, A.M. *et al.* (1999) The gene mutated in bare patches and striated mice encodes a novel 3beta-hydroxysteroid dehydrogenase. *Nat. Genet.*, **22**, 182-187.

2. McLarren, K.W., Severson, T.M., du Souich, C., Stockton, D.W., Kratz, L.E., Cunningham, D., Hendson, G., Morin, R.D., Wu, D., Paul, J.E. *et al.* (2010) Hypomorphic temperature-sensitive alleles of NSDHL cause CK syndrome. *Am. J. Hum. Genet.*, **87**, 905-914.

3. He, M., Kratz, L.E., Michel, J.J., Vallejo, A.N., Ferris, L., Kelley, R.I., Hoover, J.J., Jukic, D., Gibson, K.M., Wolfe, L.A. *et al.* (2011) Mutations in the human SC4MOL gene encoding a methyl sterol oxidase cause psoriasiform dermatitis, microcephaly, and developmental delay. *J. Clin. Invest.*, **121**, 976-984.

4. Corrales, J.D., Rocco, G.L., Blaess, S., Guo, Q. and Joyner, A.L. (2004) Spatial pattern of sonic hedgehog signaling through Gli genes during cerebellum development. *Development*, **131**, 5581-5590.

Figure S1

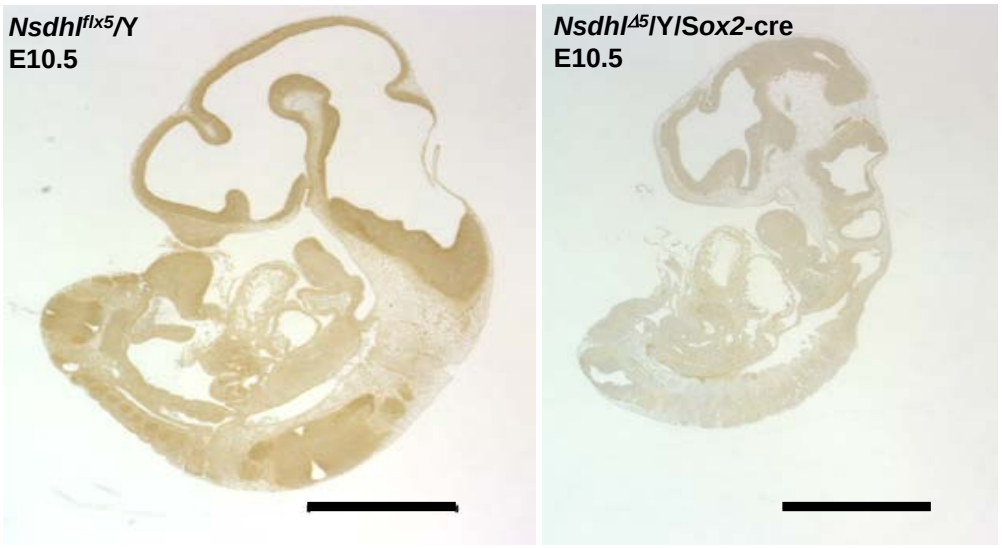
A
Nsdhl^flx5/Y
E10.5
Nsdhl^Δ5/Y/Sox2-cre
E10.5

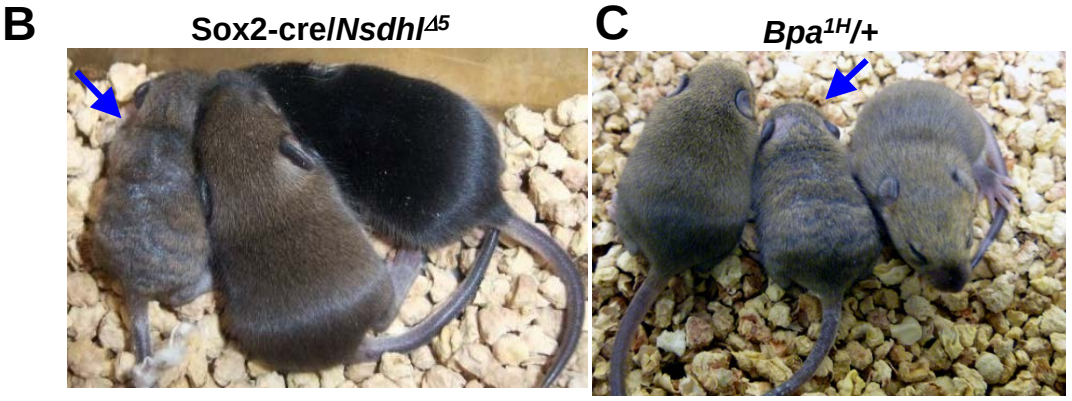
B
Sox2-cre/Nsdhl^Δ5
C
Bpa^1H/+

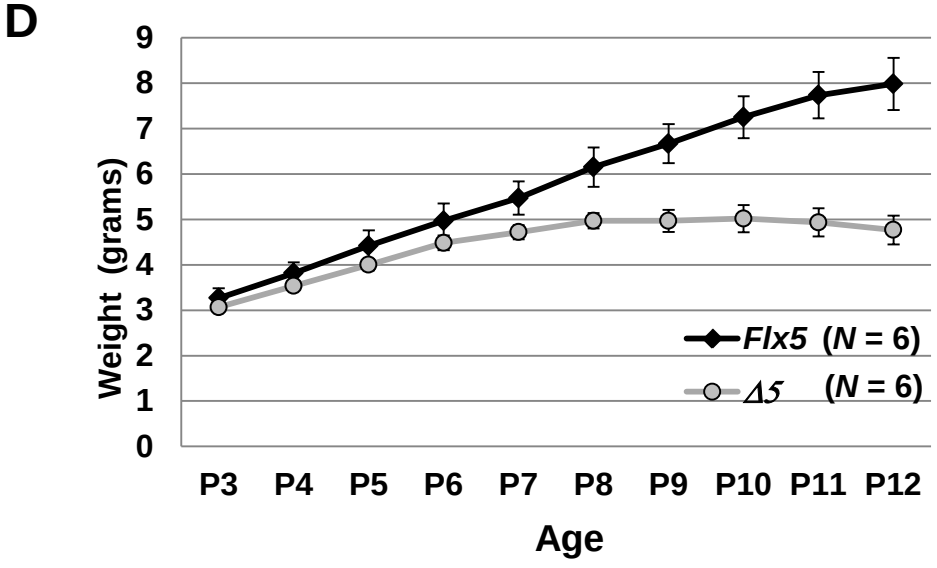
D
Weight (grams)
0
1
2
3
4
5
6
7
8
9
P3
P4
P5
P6
P7
P8
P9
P10
P11
P12
Age
Flx5 (N = 6)
Δ5 (N = 6)

Figure S2

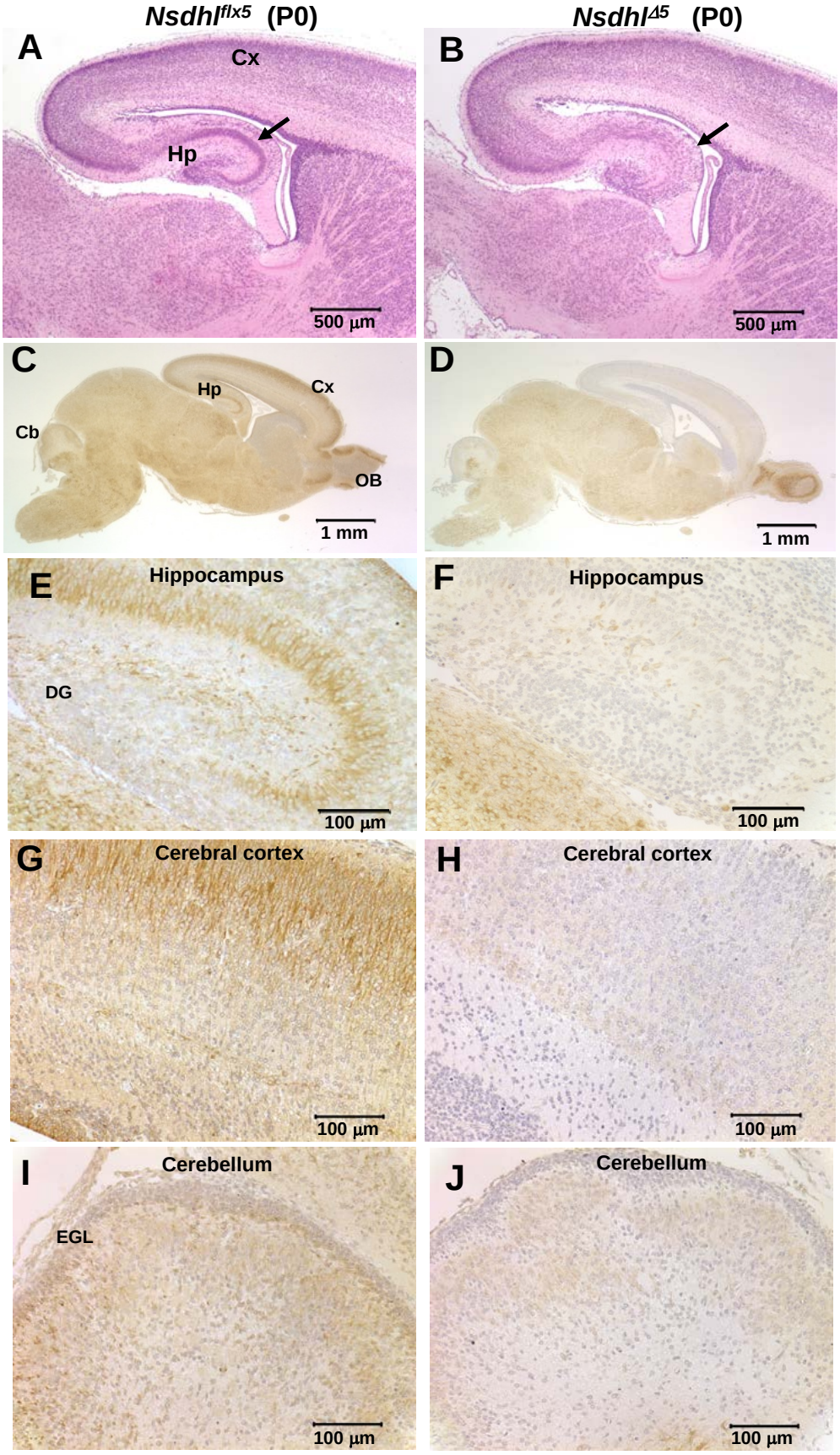
Nsdhl^flx5 (P0)
Nsdhl^Δ5 (P0)
A
Cx
Hp
500 µm
B
500 µm
C
Hp
Cx
Cb
OB
1 mm
D
1 mm
E
Hippocampus
DG
100 µm
F
Hippocampus
100 µm
G
Cerebral cortex
100 µm
H
Cerebral cortex
100 µm
I
Cerebellum
EGL
100 µm
J
Cerebellum
100 µm

Figure S3

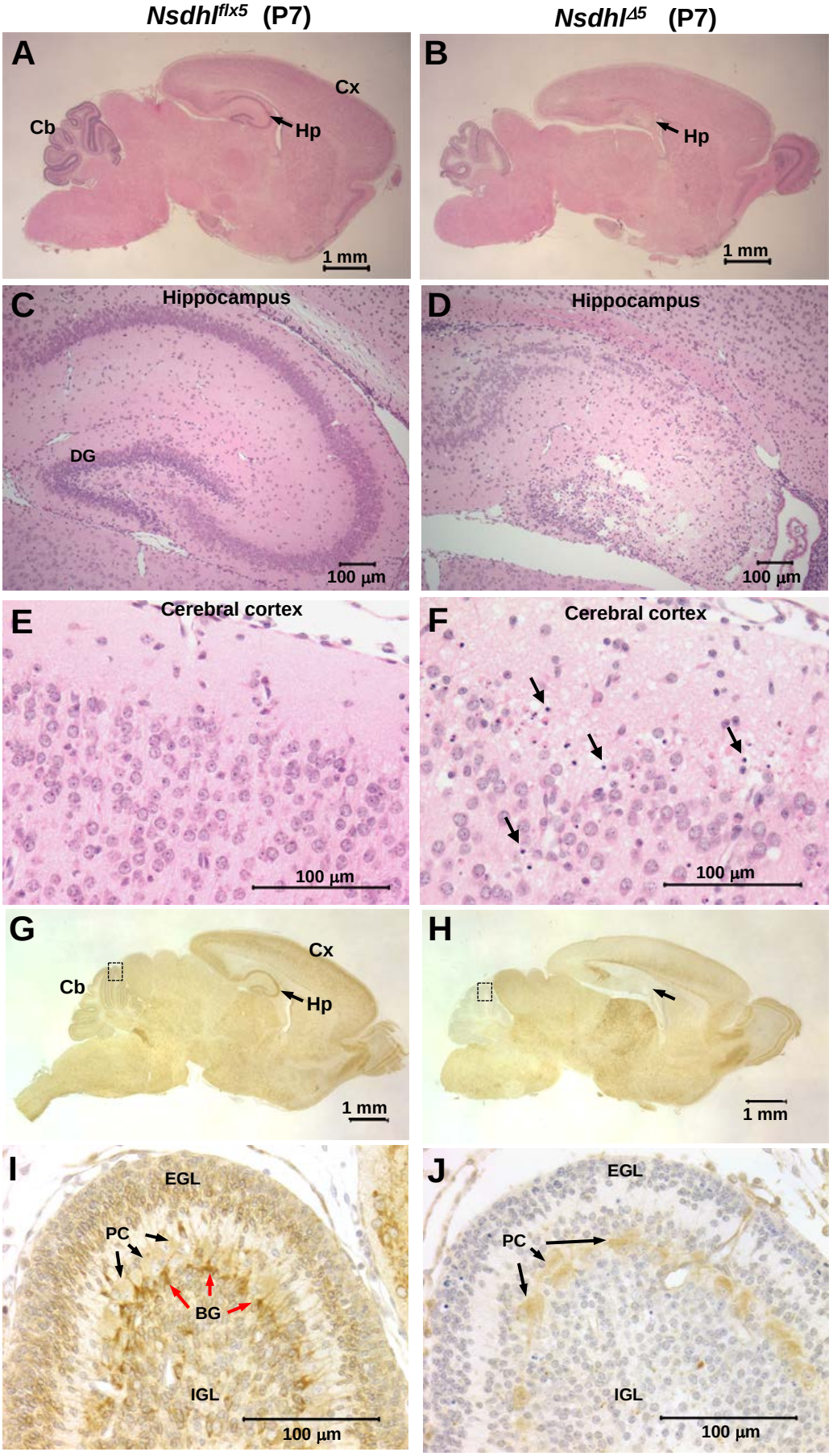
Nsdhl^flx5 (P7)
Nsdhl^Δ5 (P7)
A
Cx
Cb
Hp
1 mm
B
Hp
1 mm
C
Hippocampus
DG
100 μm
D
Hippocampus
100 μm
E
Cerebral cortex
100 μm
F
Cerebral cortex
100 μm
G
Cx
Cb
Hp
1 mm
H
1 mm
I
EGL
PC
BG
IGL
100 μm
J
EGL
PC
IGL
100 μm

Figure S4

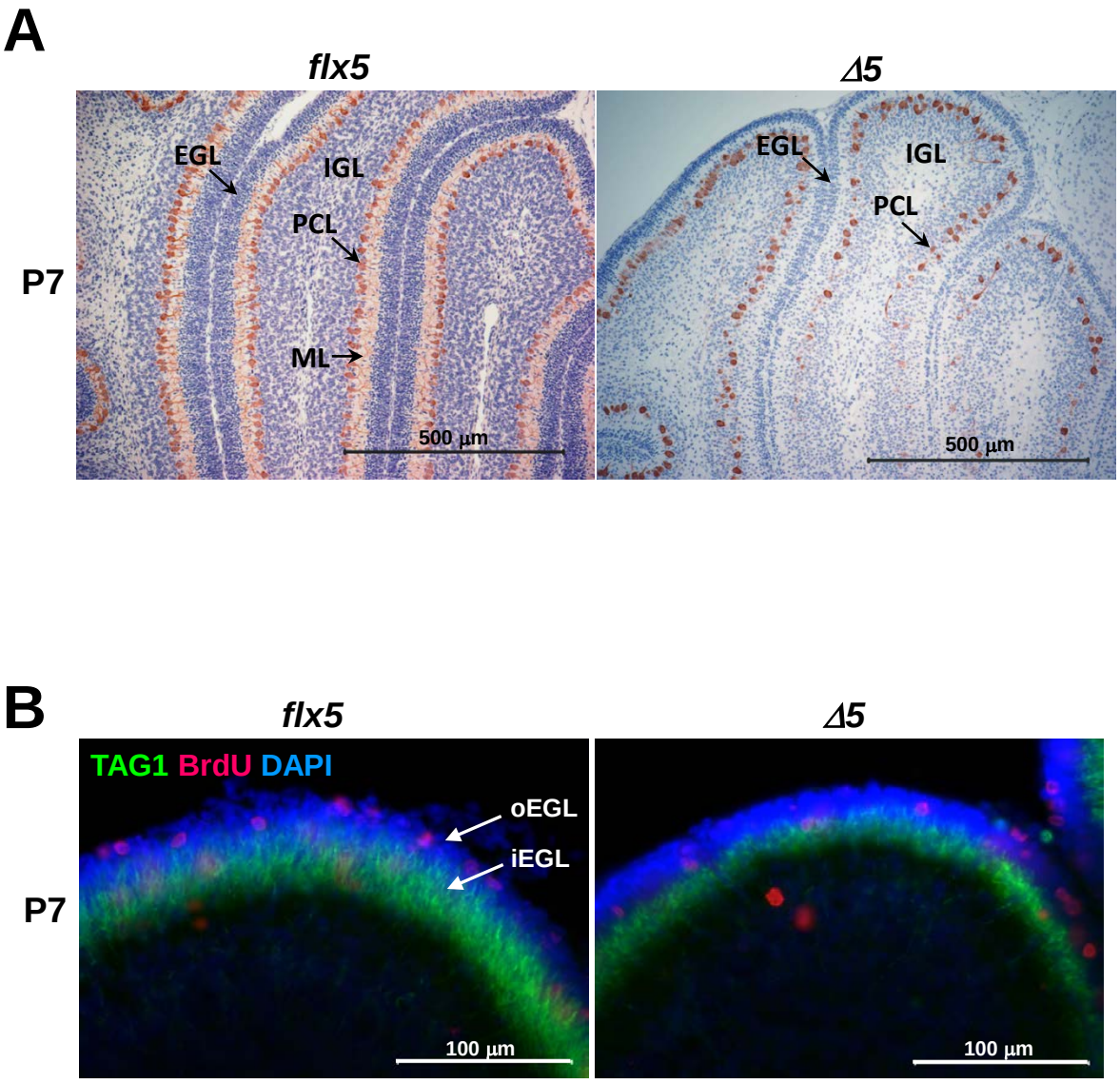
A
flx5
Δ5
P7
EGL
IGL
PCL
ML
500 µm
EGL
IGL
PCL
500 µm
B
flx5
Δ5
P7
TAG1 BrdU DAPI
oEGL
iEGL
100 µm
100 µm

Figure S4 (cont.)

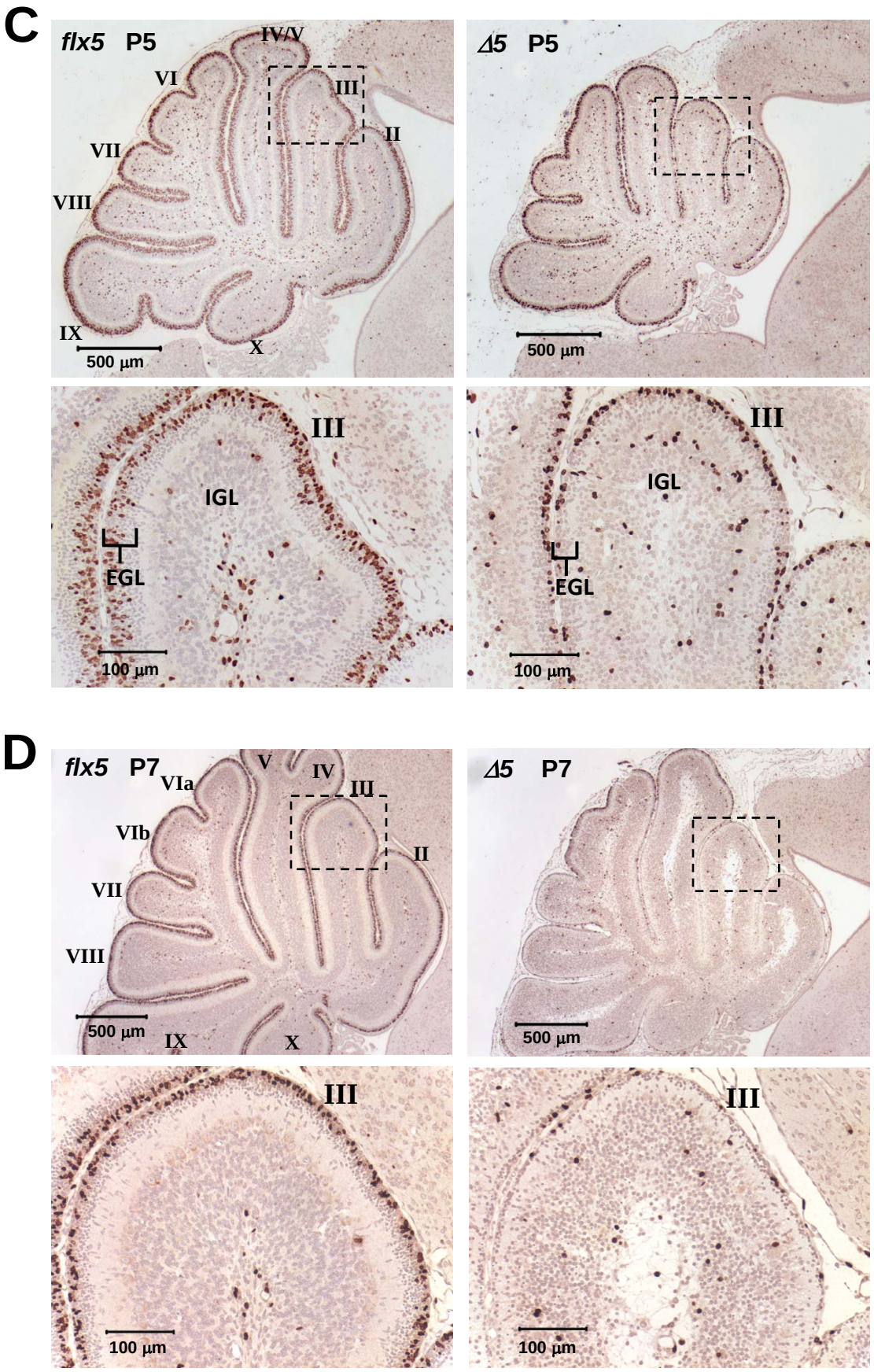

Figure S5

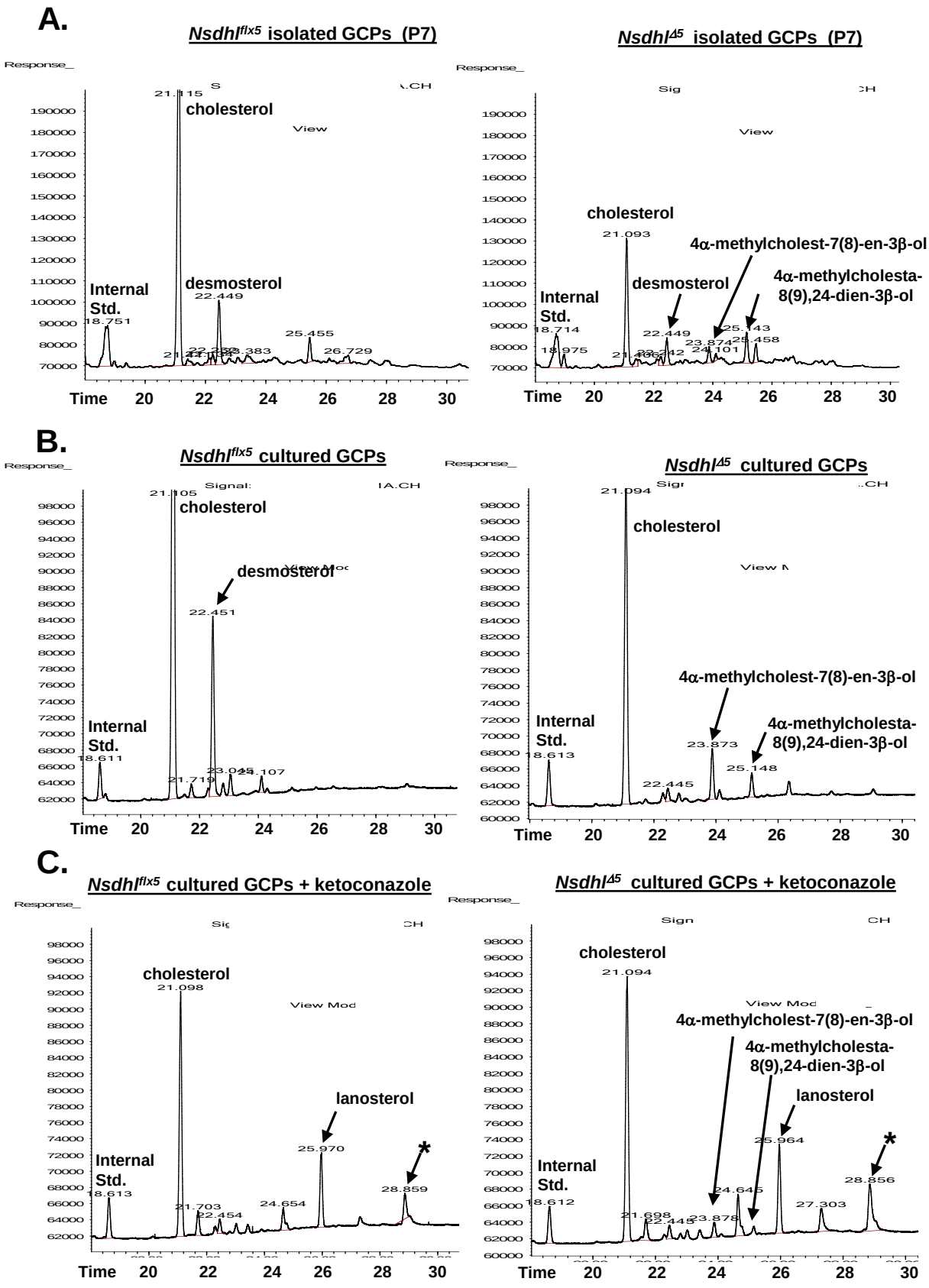
A.
Nsdhl^flx5 isolated GCPs (P7)
Nsdhl^Δ5 isolated GCPs (P7)
cholesterol
desmosterol
Internal Std.
4α-methylcholest-7(8)-en-3β-ol
4α-methylcholesta-8(9),24-dien-3β-ol
B.
Nsdhl^flx5 cultured GCPs
Nsdhl^Δ5 cultured GCPs
C.
Nsdhl^flx5 cultured GCPs + ketoconazole
Nsdhl^Δ5 cultured GCPs + ketoconazole
lanosterol
* Underivatized lanosterol

Figure S5 (cont.)

D.

Sterol analysis of isolated GCPs from *Nsdhl^{flx5}* male (P7)

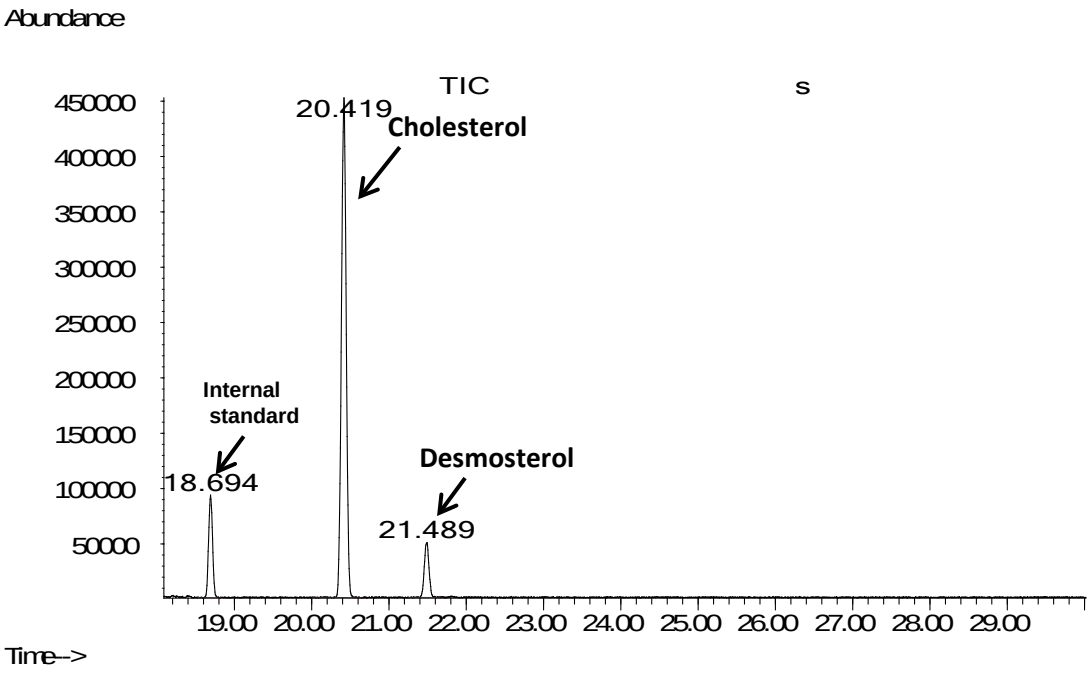

Sterol analysis of isolated GCPs from *Nsdhl$^{\Delta 5}$* male (P7)

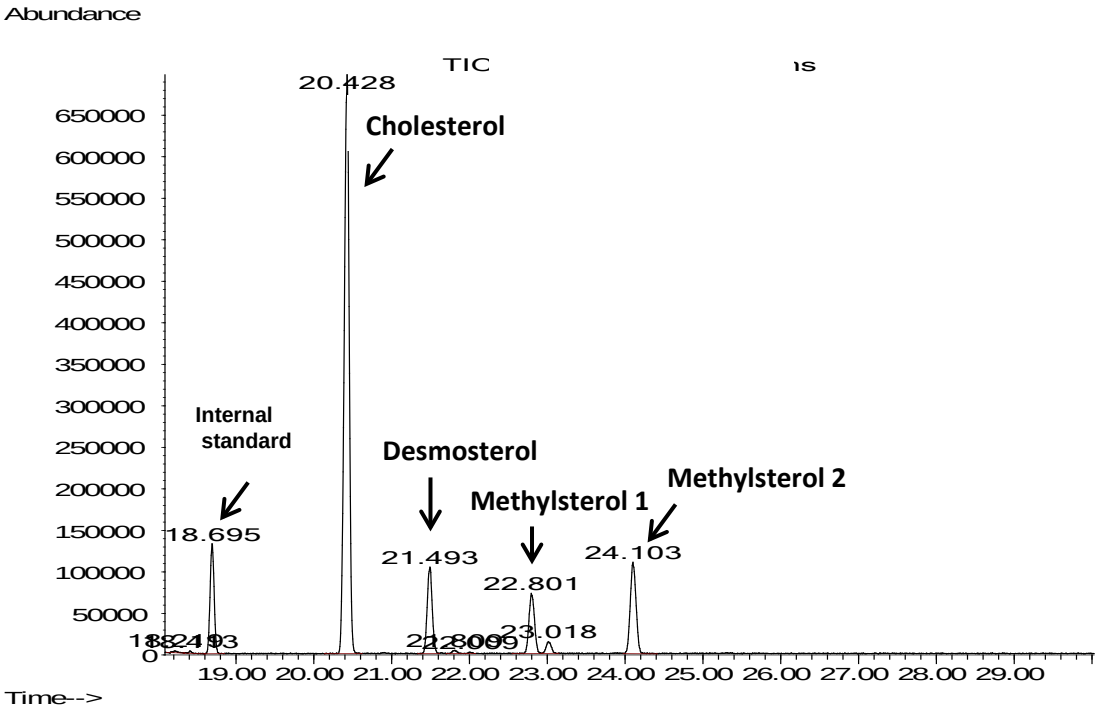

Figure S5

D. (cont.)

RT 22.8 Methylsterol 1, 4α-methylcholesta-7(8)-en-3β-ol, Match score 90

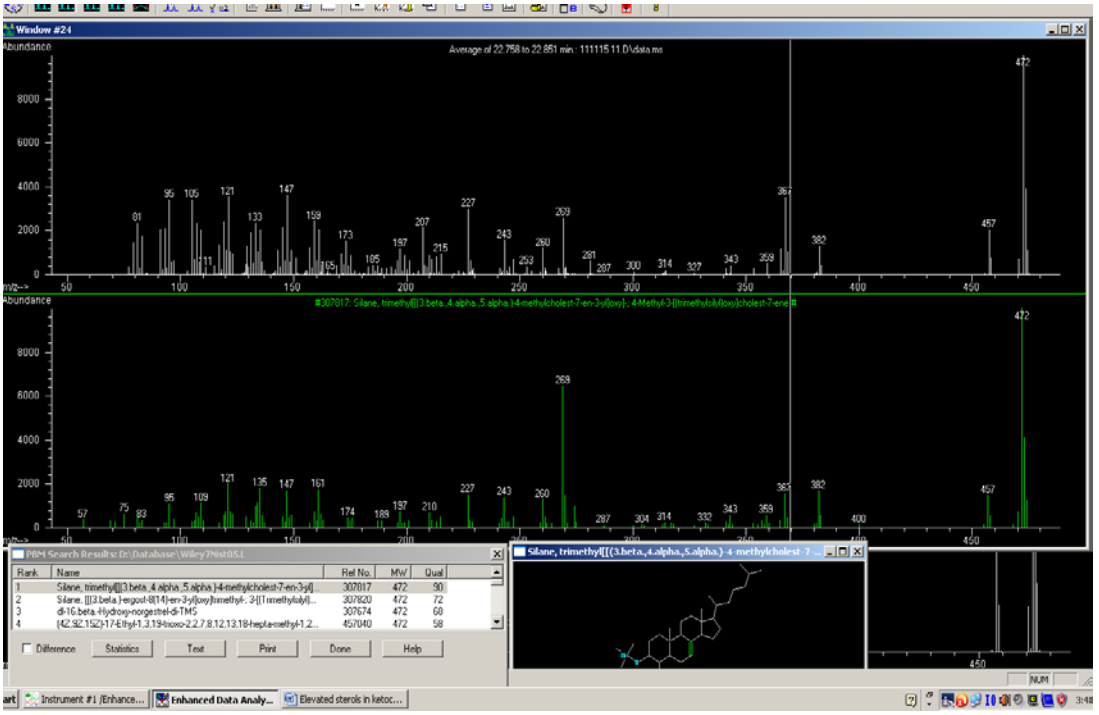

RT 24.1 Methylsterol 2, 4α-methylcholesta-8(9), 24- dien-3β-ol, Match score 92

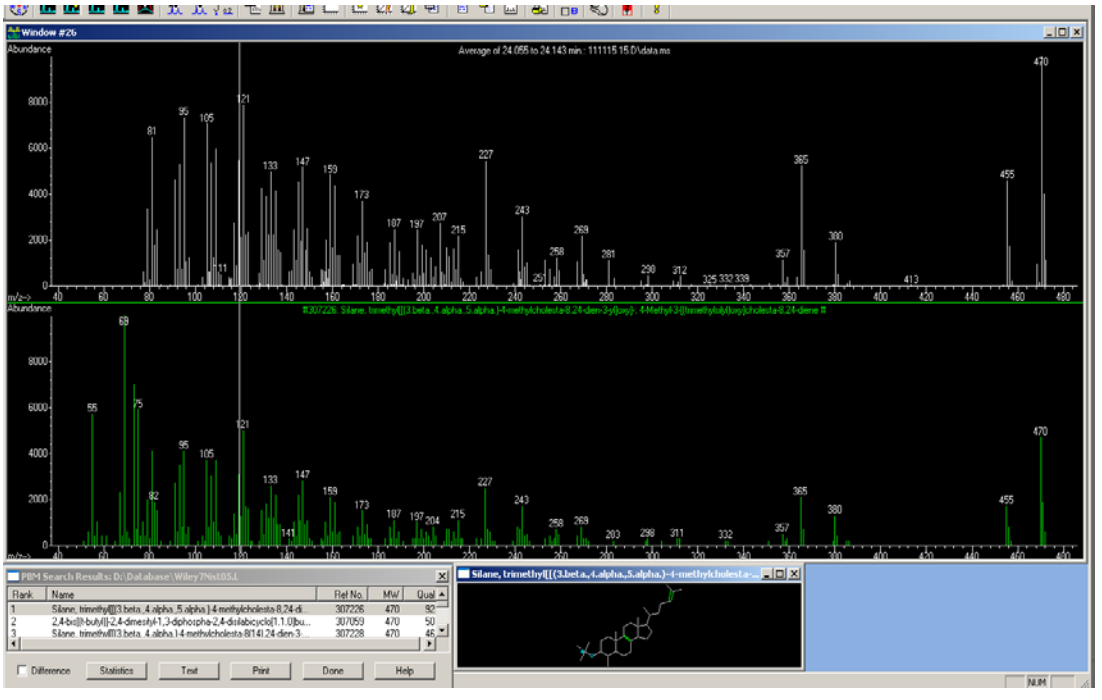

Figure S6

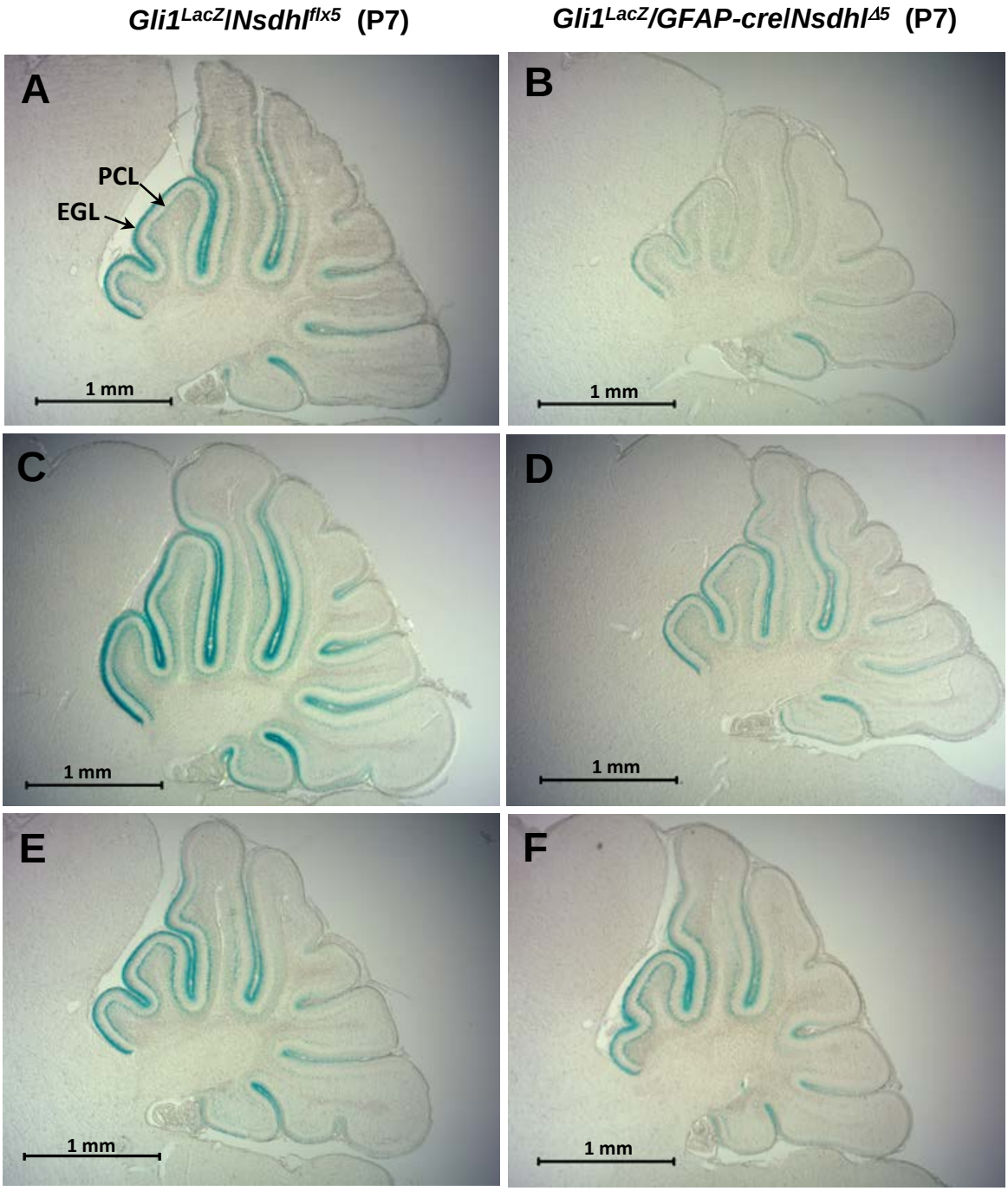
Gli1LacZ/Nsdhlflx5 (P7)
Gli1LacZ/GFAP-creNsdhlΔ5 (P7)
A
PCL
EGL
1 mm
B
1 mm
C
1 mm
D
1 mm
E
1 mm
F
1 mm

Figure S7

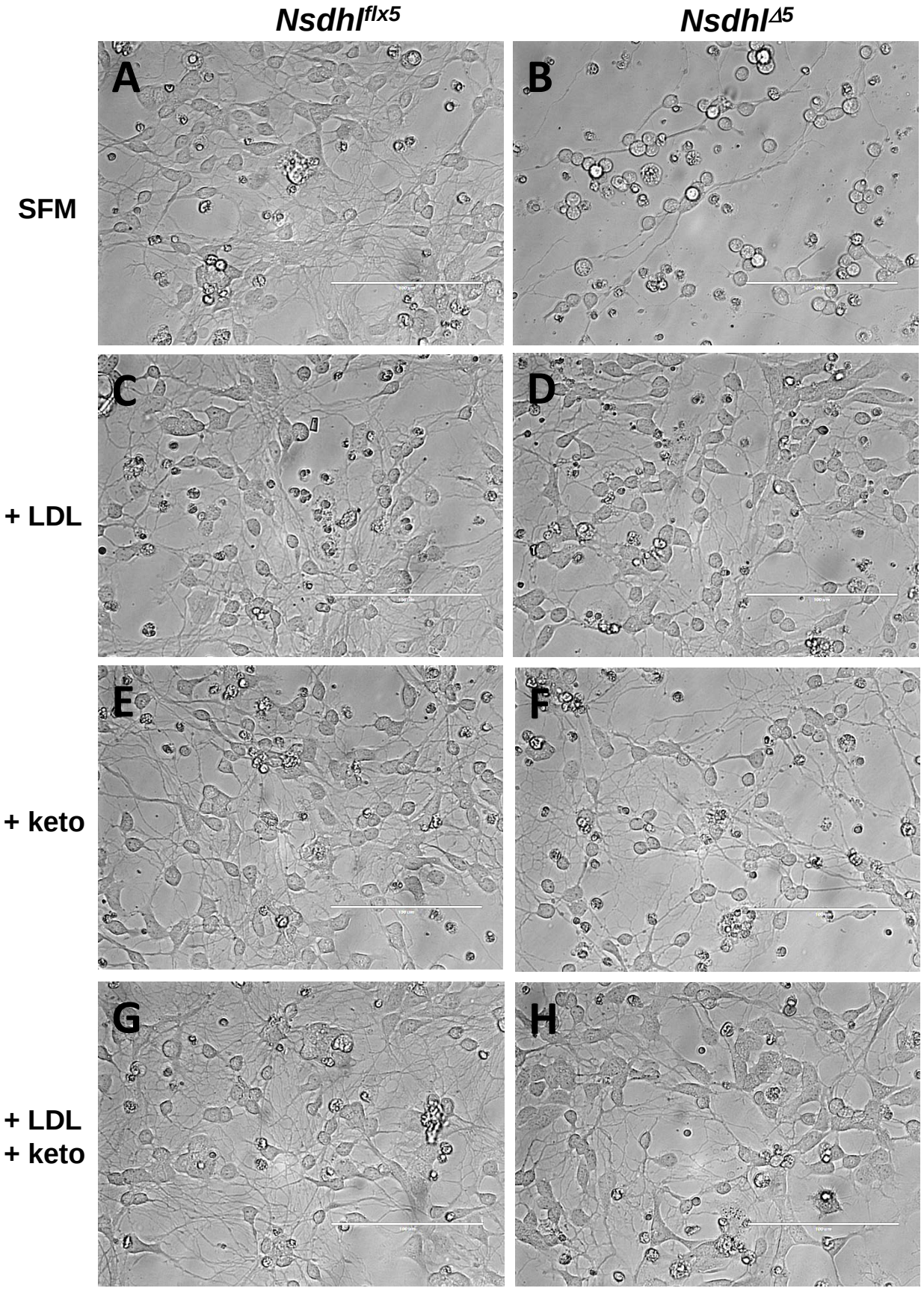

Figure S8

SFM

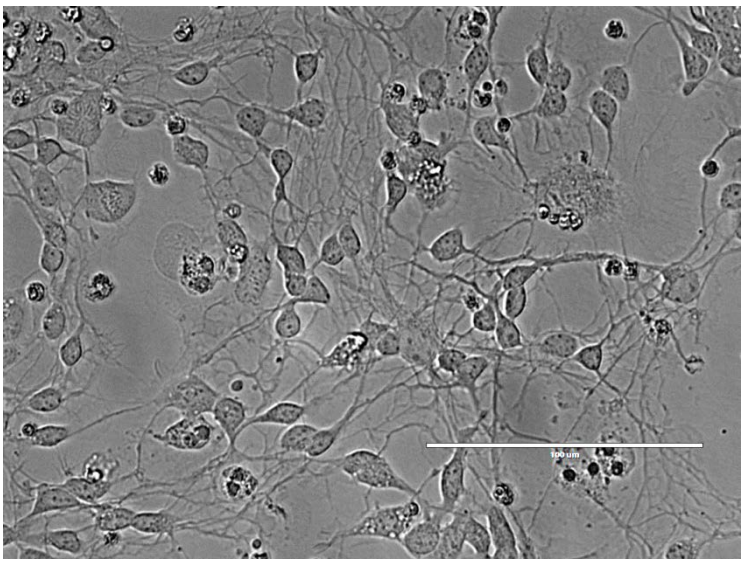

T-MAS
(2.5 μg/ml)

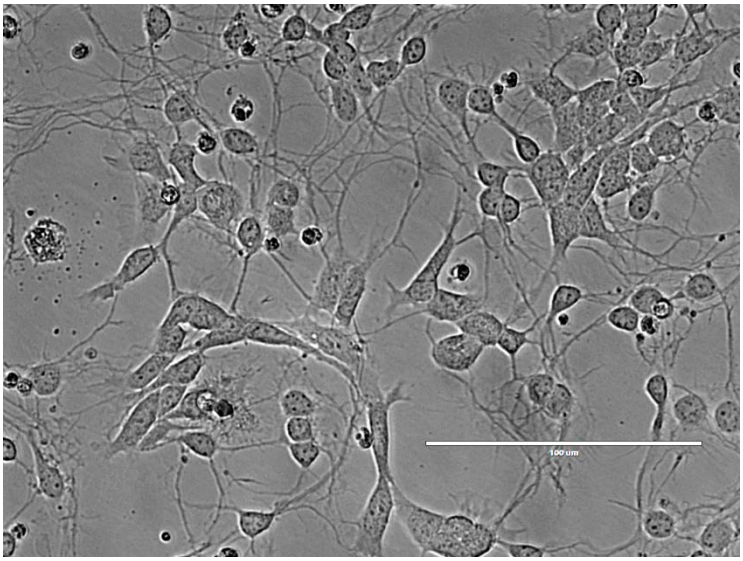

T-MAS
(10 μg/ml)

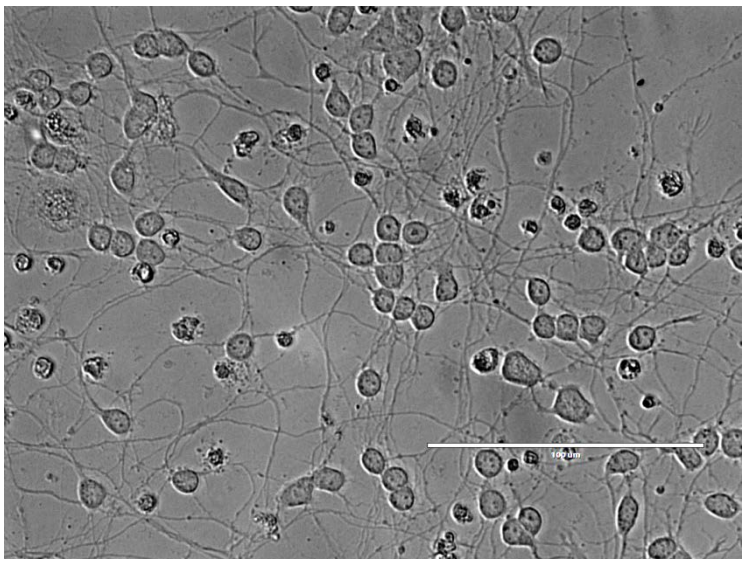

Supplementary Table 1. PCR primers.

Primer name	Sequence (5' → 3')	Annealing temp (°C)	Amplicon length (bp)	Use
Ccnd1F	TCCTCTCCAAAATGCCAGAG	60	110	qPCR
Ccnd1R	GGGTGGGTTGGAAATGAAC			
Ccnd2F	ACACACTCACGTGTGATGCC	60	98	qPCR
Ccnd2R	CAGAGCTTCGATTTGCTCCT			
CreF	GGACATGTTCAGGGATCGCCAGGCG	55	219	Genotype
CreR	CGACGATGAAGCATGTTTAGCTG			(hGFAP-cre, Sox2-cre)
GAPDHF	CGTCCCGTAGACAAAATGGT	60	110	qPCR
GAPDHR	TTGATGGCAACAATCTCCAC			
Gli1F	TACATGCTGGTGGTGCACAT	60	101	qPCR
Gli1R	CTTGAGGTTTTCAAGGCGTG			
Gli2F	GCTCAAGTCACTGAAGGATT	60	106	qPCR
Gli2R	GAAGTTTTCCAGGACAGAAC			
Gli3F	ACGAGAACAGATGTCAGCGA	60	99	qPCR
Gli3R	TGCGTTTCTTCTCTCTCGGT			
HmgcrF	TGGAATGCCTTGTGATTGGAG	60	71	qPCR
HmgcrR	AGCCGAAGCAGCACATGATC			
LacZF	ATCCTCTGCATGGTCAGGTC	55	315	Genotype
LacZR	CGTGGCCTGATTCATTCC			(*Gli1*^{LacZ})
MycnF	TCAGCACCTCCGGAGAGGAT	60	96	qPCR
MycnR	TCTCTACGGTGACCACATCG			
Nsdhlflx5F	GTGCTACTGTAGACTGAACC	55	WT = 146	Genotype
Nsdhlflx5R	TCTCCTGGATGCTCTGATAC		*flx5* = 235	
NsdhlRTF	CATTGGCACCAAGACTGTCA	60	*flx5* = 235	RT-PCR
NsdhlRTR	AGGACGAATGGCTGCGGTTA		Δ5 = 88	
Ptch1F	AATTCTCGACTCACTCGTCCA	60	104	qPCR
Ptch1R	CTCCTCATATTTGGGGCCTT			
Sc4molF	GTGGGCATGGGTGACCATAC	60	112	qPCR
Sc4molR	GTGGAAATCATGGTGCCGAG			